

## SN 2023adisy – a normal Type Ia Supernova at $z=2.9$ , discovered by *JWST*

JÓZSEF VINKÓ<sup>1,2,3,4</sup> AND ENIKŐ REGŐS<sup>1</sup>

<sup>1</sup>*HUN-REN CSFK Konkoly Observatory, Konkoly Thege M. út 15-17, Budapest, 1121, Hungary*

<sup>2</sup>*Department of Experimental Physics, Institute of Physics, University of Szeged, Dóm tér 9, Szeged, 6720 Hungary*

<sup>3</sup>*ELTE Eötvös Loránd University, Institute of Physics and Astronomy, Pázmány Péter sétány 1A, Budapest 1117, Hungary*

<sup>4</sup>*Department of Astronomy, University of Texas at Austin, 2515 Speedway, Stop C1400, Austin, TX, 78712-1205, USA*

### ABSTRACT

SN 2023adisy, a Type Ia supernova discovered by *JWST* at  $z = 2.9$ , was found to be a peculiar event, being extremely red and faint, but showing very similar rest-frame light curve decline rate to the majority of low-redshift SNe Ia. In this paper we show that the red color and faint peak magnitude could be explained by significant reddening/extinction due to dust in the host galaxy. If host galaxy extinction is accounted for, the parameters of the best-fit light curve templates in the SALT3-NIR model are compatible with a slowly declining, but still “normal” SN Ia. Comparison of the inferred luminosity distance with the prediction of the  $\Lambda$ CDM cosmology (assuming  $H_0 = 70 \text{ km s}^{-1} \text{ Mpc}^{-1}$  and  $\Omega_M = 0.315$ ) on the Hubble-diagram suggests no significant evolution of the SN Ia peak luminosity at  $z > 2$  redshifts. It is also shown that the discovery of a single SN Ia between  $2 < z < 3$  within the area of the JADES survey during 1 year is consistent with the current estimates for the SN Ia rates at such redshifts.

### 1. INTRODUCTION

Thermonuclear (Type Ia) supernovae (SNe) discovered at high ( $z > 2$ ) redshifts offer a great opportunity for testing both the cosmic star formation rate (SFR, Oda & Totani 2005; Regős & Vinkó 2019; Yan et al. 2023) as well as the nature of dark energy via the cosmological models (Lu et al. 2022). Recently, SN 2023adisy was discovered by Pierel et al. (2024, P24 hereafter) as a Type Ia SN at  $z = 2.9$  during the JADES survey (Eisenstein et al. 2023). Interestingly, P24 found that SN 2023adisy looks like a peculiar SN Ia: its light curve and spectrum suggests a normal Type Ia, but it has a very red color reminiscent of an extremely low-luminosity SN Ia (its absolute peak brightness in the B-band was found to be  $M_B \sim -16.45 \text{ mag}$ , about 3 mag lower than that of normal SNe Ia), despite its normal light curve decline rate and relatively high Ca II expansion velocity ( $\sim 18,000 \text{ km s}^{-1}$ ). P24 also pointed out that with such a faint peak brightness and red color SN 2023adisy could also be a Ca-rich SN Ia, even though it is  $\sim 1 \text{ mag}$  brighter than a typical Ca-rich event, SN 2016hmk. They noted that its peak bright-

ness is more similar to that of 91bg-like SNe Ia, but the relatively normal decline rate of its light curve is incompatible with a fast-declining 91bg-like SN. Finally, P24 found that the standardized absolute peak magnitude of SN 2023adisy is consistent with the prediction of the  $\Lambda$ CDM cosmological model assuming  $H_0 = 70 \text{ km s}^{-1} \text{ Mpc}^{-1}$  and  $\Omega_M = 0.315$ , despite its peculiarities mentioned above.

P24 argued that the Spectral Energy Distribution (SED) fitting of the host galaxy of SN 2023adisy (JADES-GS+53.13485–27.82088 indicates a low-mass ( $\sim 10^8 M_\odot$ ), low-metallicity ( $\sim 0.3Z_\odot$ ), low-extinction ( $A_V < 0.1 \text{ mag}$ ) galaxy, which suggests that the red color of the SN is probably not due to dust extinction. However, if SN 2023adisy were intrinsically so red as observed, it would be a very peculiar SN Ia, as mentioned above. Since SN 2023adisy is the first spectroscopically confirmed SN Ia beyond  $z > 2$ , its peculiar nature might imply additional possibilities about the physical differences between high and low-redshift SNe Ia.

In this paper we revisit the issue of the red color of SN 2023adisy by investigating whether it could be due to simply dust extinction within its host galaxy, even though the galaxy itself might have relatively low dust content. We re-analyze the *JWST* NIRC*am* photometry of SN 2023adisy published by P24, and examine how the parameters of the best-fit light curve templates

change if host extinction is also allowed in the model. The data and the fitting methodology is explained in Section 2, while the results are presented and discussed in Section 3.

## 2. DATA AND MODELING

We use JWST NIRCcam photometry of SN 2023adsy from P24, taken with F150W, F200W, F277W, F356W and F444W filters. Data taken with F090W and F115W are not considered, as P24 obtained only upper limits for SN 2023adsy using those filters.

The NIRCcam photometry is fitted by the SALT3-NIR light curve model (Pierel et al. 2022) that extends the spectral coverage of the SALT3 templates (Kenworthy et al. 2021) into the near-IR, up to  $\sim 2$  microns. SALT3-NIR contains Spectral Energy Distribution (SED) flux templates that are fitted to the observations using the following parameters:

- $x_0$ : the flux-scaling factor (“amplitude”) of the best-fit template;
- $x_1$ : the time-scaling factor (“stretch”) of the best-fit template;
- $c$ : the color coefficient.

Since  $x_0$  is very low ( $\sim 10^{-7}$ ) for  $z > 2$  SNe, the rest-frame  $B$ -band peak magnitude,  $m_B$ , can also be used instead of  $x_0$ . From the Pantheon+SH0ES sample (Riess et al. 2022) we found that  $m_B$  is related to  $x_0$  via  $m_B = -2.5 \log_{10}(x_0) + 10.607$ .

The peak absolute magnitude of the SN in the rest-frame  $B$ -band is calculated via the Tripp-relation (Tripp 1998) as

$$M_B = M_B^0 - \alpha x_1 + \beta c, \quad (1)$$

where  $M_B^0$  is the standardized peak absolute magnitude of the SN in the  $B$ -band,  $x_1$  and  $c$  are the best-fit SALT3 stretch and color parameters, while  $\alpha$  and  $\beta$  are the nuisance parameters that minimize the dispersion of the SNe Ia measurements on the Hubble-diagram. In this study we adopt  $M_B^0 = -19.253$  (Riess et al. 2022),  $\alpha = 0.148$  and  $\beta = 3.09$  (Brout et al. 2022), which are based on the analysis of the Pantheon+ and SH0ES samples. Finally, from the best-fit parameters, the distance modulus of the SN is given by

$$\mu = m_B - M_B = m_B - M_B^0 + \alpha x_1 - \beta c. \quad (2)$$

Note that in Equation (2) we ignore the bias-correction term  $\delta_B$  (Kessler & Scolnic 2017), since SN 2023adsy turns out to be redder than the majority of the normal SNe Ia (see Section 3), while  $\delta_B$  is more important for bluer SNe Ia (Kessler & Scolnic 2017).

Pierel et al. (2024) also found that for SN 2023adsy  $\delta_B$  is negligibly small.

Per definition, the SALT3 model does not contain information on extinction/reddening from dust either in the Milky Way, or within the host galaxy. In the NIR the Milky Way extinction is relatively low for extragalactic objects, at least compared to the optical extinction, thus, it can be ignored for the NIRCcam bands. On the other hand, for  $z > 2$  SNe, the observer-frame NIR corresponds to rest-frame optical bands, thus, extinction within the host galaxy may be significant. Since the  $c$  parameter contains a mixture of both the SN intrinsic color and the reddening due to dust extinction, it is not easy to decide whether we see a peculiar SN Ia that is redder than the normal ones, or it is a normal, but heavily reddened SN Ia.

Even though the intrinsic color and dust reddening are highly correlated, still, it might be possible to disentangle the two effects if one takes into account the expected distribution of “normal” SNe Ia on the color-stretch ( $c$ - $x_1$ ) diagram as a prior for these parameters. Therefore, in this study we add host galaxy extinction with the usual  $E(B - V)_{\text{host}}$  parameter to modify the SALT3-NIR templates in rest-frame. This is a slightly modified model compared to that of P24, who mixed the effect of host extinction with the intrinsic SN color, and applied a single  $c$  parameter in their fitting.

The synthetic light curves in NIRCcam bands from the SALT3-NIR templates are computed within the `sncosmo`<sup>1</sup> Python environment (Barbary et al. 2016). Two slightly different models are implemented to fit the observed data: in Model A we use  $\log_{10}(x_0)$  as a free fitting parameter (within bounds, see below) independently from  $x_1$  and  $c$ , while in Model B we apply Equation (1) to constrain  $M_B$  via  $x_1$  and  $c$ . In the latter case the distance modulus, which is needed to fit the synthetic light curves to the data, is calculated directly from redshift via a cosmological model, for which we adopt a flat  $\Lambda$ CDM model with  $H_0 = 70.0 \text{ km s}^{-1} \text{ Mpc}^{-1}$  and  $\Omega_M = 0.315$  (same as in P24). In Model B the fitting parameters are  $x_1$ ,  $c$ ,  $E(B - V)_{\text{host}}$  and  $dt_{\text{max}}$  (the difference between the observed moment of  $B$ -band maximum and a fixed, but arbitrary reference epoch), while they are  $\log_{10}(x_0)$ ,  $x_1$ ,  $c$ ,  $E(B - V)_{\text{host}}$  and  $dt_{\text{max}}$  in Model A.

For computing the fitting via  $\chi^2$  minimization, we apply the Price algorithm (Brachetti et al. 1997; Chatzopoulos et al. 2013), a controlled random-search technique that uses  $N > 100$  realizations of the model, each having different parameter values (within their pre-

<sup>1</sup> <https://github.com/sncosmo/sncosmo>

defined bounds), and shifts them toward the location of the absolute minimum within the bounded volume of the  $\chi^2$  hyperspace via a Monte-Carlo iteration process. We use  $\Delta\chi^2/\chi_{\min}^2 \leq 0.1$  as the stopping criterion for the iteration, where  $\Delta\chi^2 = \chi_{\max}^2 - \chi_{\min}^2$  for the  $N$  different model realizations. Since the geometry of the  $\chi^2$  hypersurface can be quite complex, we define the best-fit value of each parameter as the median of that particular parameter of the  $N$  random models after they reached the stopping criterion, instead of using exclusively the model with the lowest  $\chi^2$ . The distribution of the same random models around the minimum are used to estimate the uncertainty of each best-fit parameter value.

The parameter bounds, which define the search volume in the parameter space, are defined similar to P24:  $\log_{10}(x_0) = [-9, -5]$ ,  $x_1 = [-3, 3]$ ,  $c = [-1.5, 1.5]$ ,  $E(B - V)_{\text{host}} = [0, 2]$ ,  $dt = [-10, 10]$ . The reference epoch is set to  $t_0 = 60240.0$ , which is close to the best-fit peak time found by P24.

### 3. RESULTS AND DISCUSSION

This section contains the SALT3-NIR model fitting results and their discussion.

#### 3.1. SALT3-NIR fitting

The best-fit parameters of Model A and B, as well as the solution found by P24, are collected in Table 1. The uncertainties, inferred as the standard deviation of the distribution of the feasible models (see Section 2), are given in parentheses.

Corner plots for the best-fit parameters of Model A and B are shown in Figure 1 and 2, respectively. As expected, in Model A the flux-scaling factor ( $x_0$ ) strongly correlates with both the color term ( $c$ ) and the host reddening ( $E(B - V)_{\text{host}}$ ). This results in an especially wide distribution of the possible values of the color term: the feasible models with  $\chi^2 \leq 1.1\chi_{\min}^2$  have their color term in between  $0.1 \lesssim c \lesssim 0.5$ .

The resulting light curves from Model A (solid curves) and Model B (dashed curves) together with the NIRCam photometry of SN 2023adysy (filled circles) are shown in the left panel of Figure 3. For comparison, we also plot the best-fit light curves of P24 (dash-dotted curves). It is seen that the differences between the light curves from Model A and B are negligibly small. The differences between our best-fit light curves and those of P24 are also relatively minor, and all model light curves fit the observed data quite well. This is also reflected by the low  $\chi^2$  values of the best-fit solutions shown in Table 1. The slightly higher  $\chi^2$  of the P24 solution is caused by the F444W filter data, which could be fitted somewhat worse with their model compared to ours. Note that

due to the same reason Pierel et al. (2024) discarded the F444W data from their fitting.

In the right panel of Figure 3 the location of the best-fit parameters are shown on the  $x_1 - c$  plane for each model. Our Model A and B are plotted with filled circles, while the solution found by P24 is represented by the open circle. The grey symbols correspond to the SNe Ia in the Pantheon+ sample (Scolnic et al. 2022). It is clear that SN 2023adysy is somewhat off from the distribution of the bulk of SNe Ia on this diagram, but our best-fit solutions (Model A and B) are less extreme than the result by P24. For Model A, the best-fit stretch and color ( $x_1$  and  $c$ ) parameters are near the edge of the distribution of the SNe Ia in the Pantheon+ sample. The result from Model B is similar, but slightly more stretched and redder compared to the result from Model A.

In contrast, the solution by P24 represents a less stretched (close to  $x_1 \sim 0$ ), but very red ( $c \sim 0.9$ ) SN Ia. Such a SN Ia, having a very red color but a normal decline rate would be quite unusual, at least among the low- $z$  SN Ia sample. P24 also pointed out that their result, if true, suggests that SN 2023adysy would be peculiar: it is a normal Ia according to the light curve decline rate, a 91bg-like Ia according to its B-band absolute magnitude, but similar to a Ca-rich transient according to its very red color and Ca II velocity, even though it is  $\sim 1$  mag brighter at peak than most Ca-rich transients.

The new solutions presented in this paper (both Model A and B) suggest that this is not necessarily the case. Instead of being such a peculiar object having “mixed” properties of low- $z$  transients, SN 2023adysy could be more similar to normal low- $z$  SNe Ia, even though it is near the edge of their parameter distribution. Based on both its new best-fit stretch and color (see Table 1, SN 2023adysy would have passed the selection criteria of being a “normal” SN Ia that can be used e.g. for cosmological analysis, if it had been a low- $z$  object (Scolnic et al. 2018). Note that the new stretch parameter, which is definitely high but not extreme, might still be somewhat overestimated, because, as seen in the left panel of Figure 3, the NIRCam photometry does not cover the 2nd peak in the reddest filters, which would be the best constraint for the stretch parameter. Still, SN 2023adysy could be a “normal” SN Ia at  $z \sim 2.9$ , instead of being a peculiar object suggested by the results of P24, if most of its extremely red color is due to reddening/extinction in its host galaxy.

#### 3.2. SN 2023adysy on the Hubble-diagram

The position of SN 2023adysy on the Hubble-diagram is presented in Figure 4, together with the SNe Ia

$dt_{\max}$ (day)	$\log_{10}(x_0)$	$x_1$	$c$	$E(B - V)_{\text{host}}$ (mag)	$m_B$ (mag)	$M_B$ (mag)	$\mu$ (mag)	$\chi^2$	ref.
8.81(0.73)	-7.04 (0.19)	2.11 (0.44)	0.30 (0.13)	0.68 (0.11)	28.20 (0.48)	-18.63 (0.40)	46.83 (0.22)	1.9685	Model A
8.82 (0.66)	-7.29 (—)	2.39 (0.31)	0.47 (0.08)	0.54 (0.06)	28.83 (0.26)	-18.16 (0.26)	47.00 (0.26)	1.9543	Model B
-0.02 (1.60)	-8.15 (0.05)	-0.11 (1.04)	0.92 (0.05)	0.00 (—)	30.73 (0.15)	-16.45 (0.32)	47.18 (0.28)	6.4655	P24

**Table 1.** Best-fit parameters from the SALT3-NIR templates. Uncertainties are shown in parentheses.

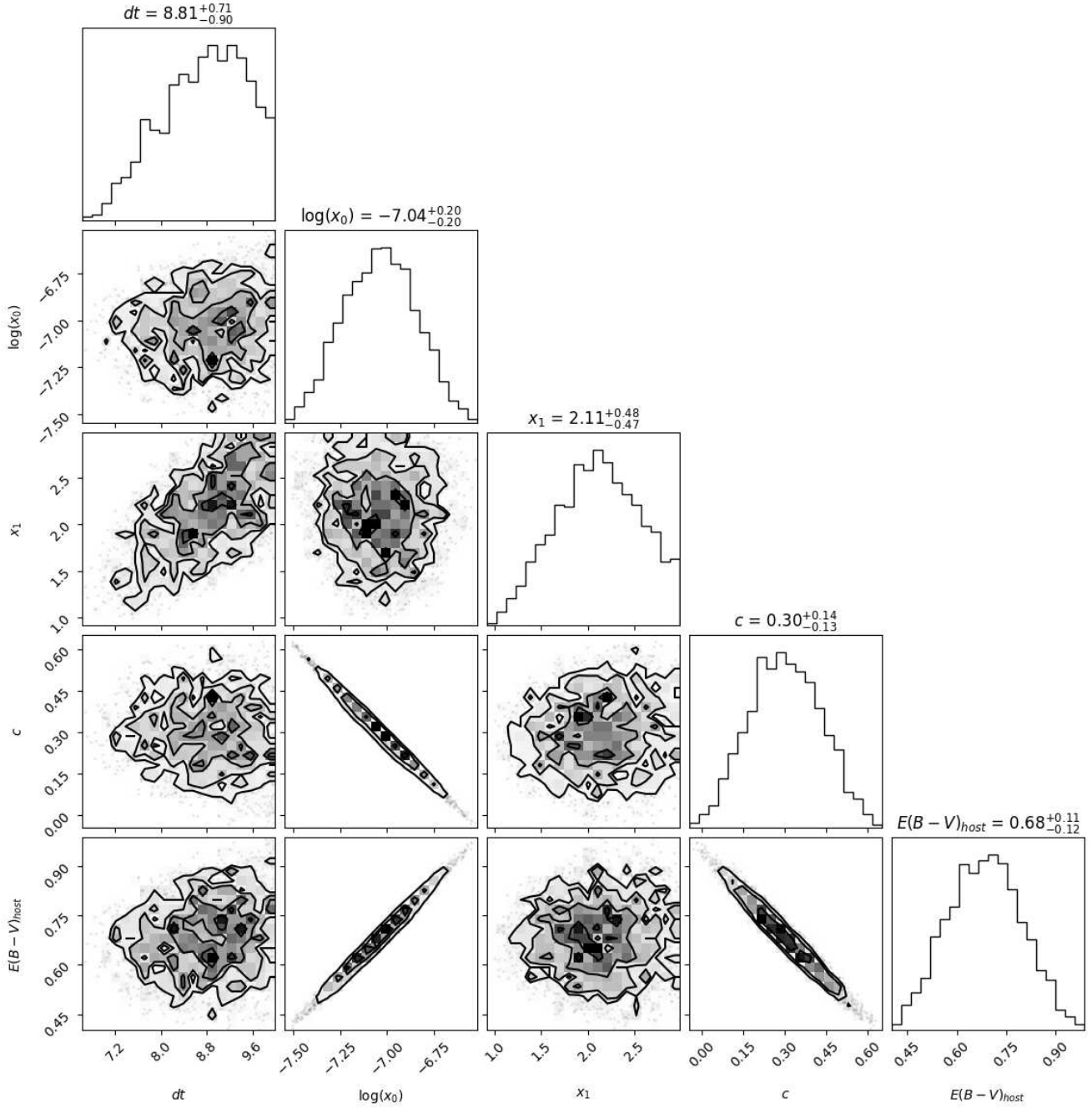


**Figure 1.** Corner plot showing the distribution of fitting parameters for Model A.

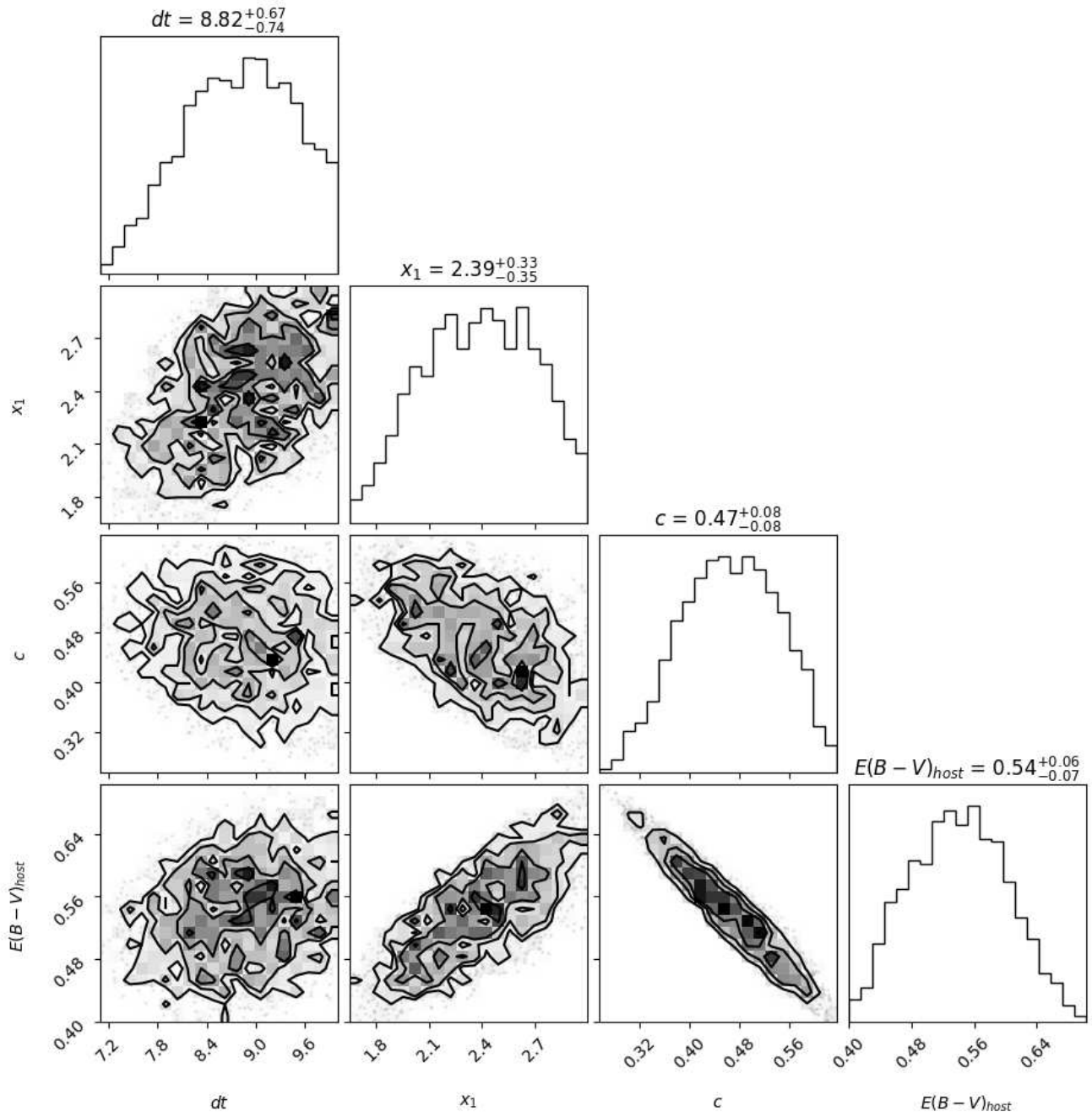
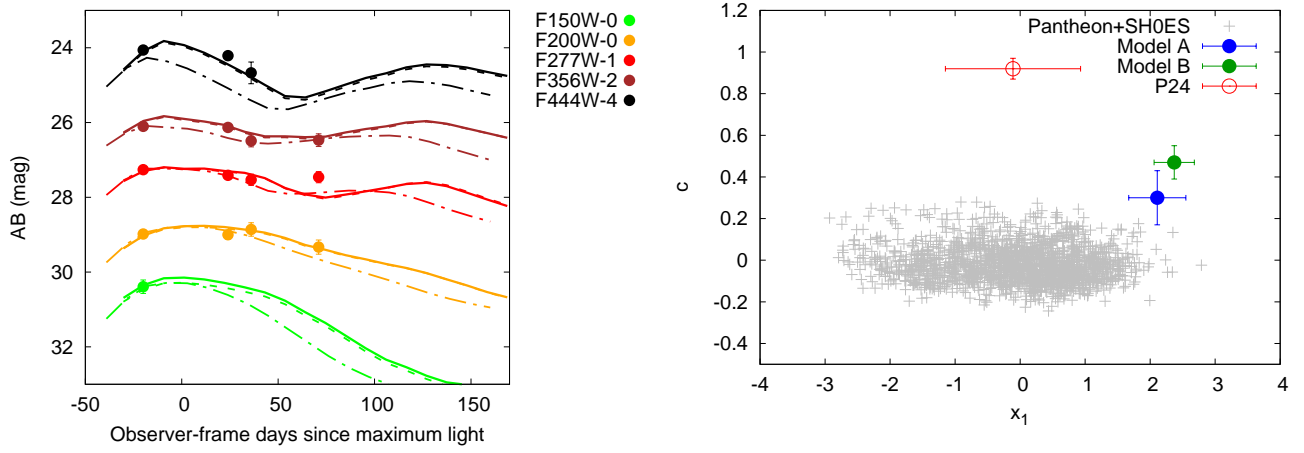
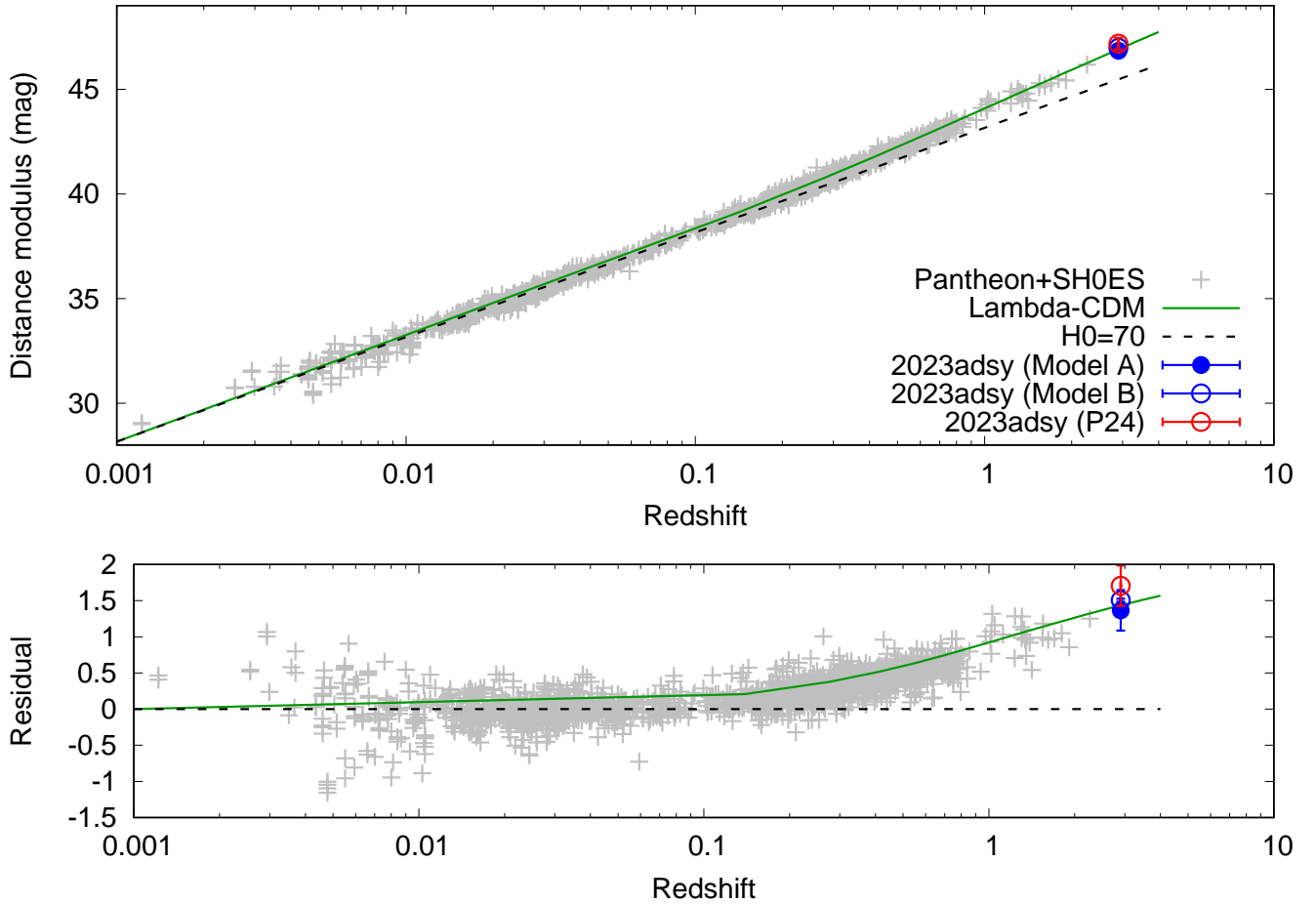


Figure 2. Same as Figure 1 but for Model B.





**Figure 3.** Left panel: the NIRCcam photometric data for SN 2023adsy (circles) and the best-fit SALT3-NIR templates (curves). Solid curves: Model A; dashed curves: Model B; dash-dotted curves: P24. The applied vertical shifts (in magnitudes) for better visibility are indicated in the legends. Right panel: The best-fit SALT parameters for SN 2023adsy (filled circles) compared to those from P24 (open circle) and other normal Type Ia SNe from the Pantheon+ sample (grey plus signs).



**Figure 4.** Hubble-diagram for SNe Ia, including SN 2023adsy. Line indicates the flat  $\Lambda$ CDM model with  $\Omega_M = 0.3$ .

from the Pantheon+SH0ES sample (Scolnic et al. 2022; Riess et al. 2022). The prediction from the adopted  $\Lambda$ CDM cosmology (Section 2) and a simple linear Hubble-law having  $H_0 = 70 \text{ kms}^{-1}\text{Mpc}^{-1}$  are also shown as solid and dashed lines, respectively. It is seen that the inferred distance modulus from both Model A and B is consistent with the prediction of the adopted  $\Lambda$ CDM model ( $\sim 46.98 \text{ mag}$ ), just like the best-fit solution of P24, at the  $1\sigma$  level.

The detection of a single SN Ia at  $z > 2$  is not sufficient to constrain the physics of the Ia population at high redshifts, but the agreement between the inferred peak luminosity of SN 2023adsy and the prediction of the  $\Lambda$ CDM cosmology fitted to low-redshift SNe Ia suggests no significant evolution of the physics of SNe Ia up to  $z \sim 3$ .

### 3.3. Constraints on the SN Ia rates and Delay-Time Distributions at high- $z$

Following Regős & Vinkó (2019), we estimate the expected numbers of SNe Ia within the JADES survey area as a function of redshift, and compare these predictions with the discovery of a single event, SN 2023adsy.

The expected number of SNe Ia at a given redshift depends on two quantities: the Cosmic Star Formation Rate (SFR) and the Delay Time Distribution (DTD), both as a function of redshift. Regős & Vinkó (2019) considered a variety of proposed DTD functions and computed different predictions for the numbers of SNe Ia at  $z > 1$ . Here we use their Table 2, which shows the numbers for the single-degenerate (SD) and double-degenerate (DD) scenarios, as well as the mixed “prompt+DD” scenario by Rodney et al. (2014). Since those numbers correspond to a different survey area ( $300 \text{ arcmin}^2$  instead of 25) and a 3 year-long survey time, we rescale them to the area of the JADES survey and 1 year survey time. The results are shown in Table 2 and plotted in Figure 5. The right panel displays the numbers that were inferred after assuming a  $\sim 30$  day-long visibility time in the rest frame for each event, which are given in the  $N_{30}$  columns in Table 2.

The numbers in Table 2 suggest that within the redshift interval of  $1 < z < 2$  the number of SNe Ia that are detectable within the JADES survey area during 1 year are 3.0, 3.4 and 3.5 for the SD, DD and R14 scenarios, respectively, while between  $2 < z < 3$  these are 2.5, 3.4 and 3.0. Since in these redshift intervals SNe Ia are not expected to be visible for 1 year, a more realistic estimate could be obtained from the  $N_{30}$  numbers that take into account the limited ( $\sim 30$  days in rest-frame) visibility of a SN Ia at  $z > 1$ . Using these estimates one can get 0.6, 0.7 and 0.7 SNe per year for  $1 < z < 2$  and

0.7, 1.0 and 0.9 SNe per year for  $2 < z < 3$ . The latter numbers are all consistent with the discovery of only 1 SN Ia, SN 2023adsy at  $z \sim 2.9$ . The lack of detection of a similar event at  $z < 2$  may be simply due to the lower number of potential host galaxies in this redshift interval within the JADES survey area.

Unfortunately, from a single SN Ia it is not possible to get a realistic constraint on the different DTD scenarios. Still, the discovery of SN 2023adsy with *JWST* demonstrated the possibility of detecting Type Ia SNe at significantly higher redshifts than before, which could lead to further unprecedented discoveries regarding the progenitors of SNe Ia as well as their cosmological implications in the near future.

## 4. SUMMARY

We re-fitted the NIRCcam photometry of SN 2023adsy, a Type Ia SN discovered by *JWST* at  $z \sim 2.9$  (Pierel et al. 2024), with SALT3-NIR templates taking into account a potential extinction due to dust in the host galaxy. It is found that SN 2023adsy can be adequately fitted ( $\chi^2/\text{dof} \sim 2$ ) with the SALT3-NIR model if  $E(B - V)_{\text{host}} \lesssim 0.7 \pm 0.1 \text{ mag}$  reddening due to dust is added. This resulted in a slowly declining ( $x_1 \gtrsim 2.1 \pm 0.4$ ) and moderately red ( $c \gtrsim 0.3 \pm 0.1$ ) SN Ia, which is still within the parameter distribution of “normal” SNe Ia, as shown by the Pantheon+ sample.

Our result implies that SN 2023adsy may not be such an extremely red and faint, but slowly declining and high-velocity SN Ia as found by P24, which, if true, would be a very peculiar object. The present result suggests that SNe Ia at  $z \lesssim 3$  could be more-or-less similar to their local counterparts, and their light curves can be standardized using the same techniques that work for local SNe Ia.

The Ia discovery rate from the JADES survey, 1 confirmed SN Ia in  $2 < z < 3$  per year, is consistent with the expected SN Ia rates at this redshift range. Even though a single event cannot constrain the different DTD models, more discoveries in the near future can significantly improve our understanding of the physics of SNe Ia.

This research is supported by NKFIH-OTKA grant K142534 from the National Research, Development and Innovation Office, Hungary. The SN group at Konkoly Observatory was supported by the project “Transient Astrophysical Objects” GINOP 2.3.2-15-2016-00033 by the Hungarian Government, funded by the European Union.

*Software:* sncosmo (Barbary et al. 2016), corner (Foreman-Mackey 2016)

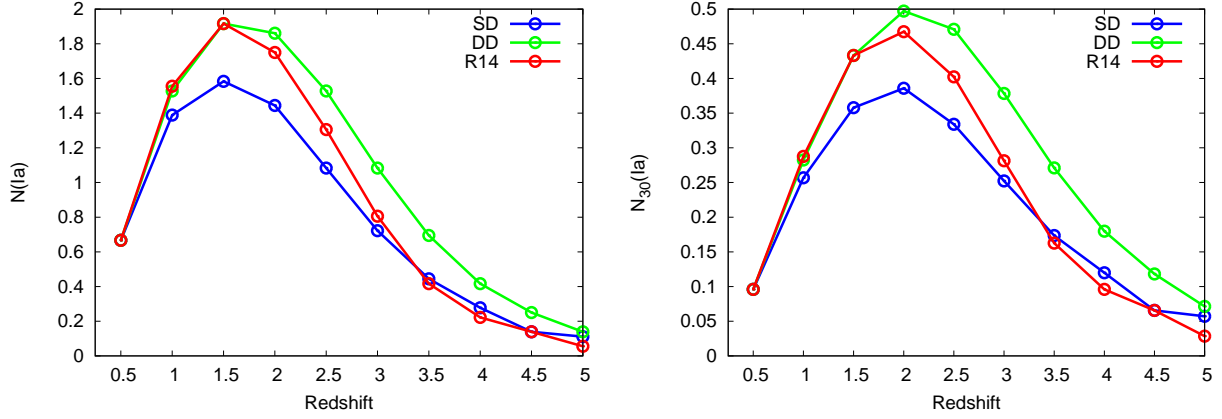


**Figure 5.** The expected number of SNe Ia as a function of redshift in the JADES survey area ( $\sim 25$  arcmin<sup>2</sup>) in 1 year (left panel). Different DTD scenarios are shown with different colors as indicated in the legend: SD = single degenerate, DD = double degenerate, R14 = Rodney et al. (2014). The right panel shows the expected numbers assuming  $\sim 30$  days rest-frame visibility time for a SN Ia.

$z$	$z+dz$	$N(\text{SD})$	$N_{30}(\text{SD})$	$N(\text{DD})$	$N_{30}(\text{DD})$	$N(\text{R14})$	$N_{30}(\text{R14})$
0.5	1.0	0.666	0.096	0.666	0.096	0.666	0.096
1.0	1.5	1.389	0.257	1.528	0.282	1.555	0.287
1.5	2.0	1.583	0.358	1.917	0.433	1.917	0.433
2.0	2.5	1.444	0.386	1.861	0.497	1.750	0.467
2.5	3.0	1.083	0.334	1.528	0.471	1.305	0.402
3.0	3.5	0.722	0.252	1.083	0.378	0.805	0.281
3.5	4.0	0.444	0.173	0.694	0.271	0.417	0.163
4.0	4.5	0.278	0.120	0.417	0.180	0.222	0.096
4.5	5.0	0.134	0.066	0.250	0.118	0.139	0.065
5.0	5.5	0.111	0.057	0.139	0.071	0.055	0.028

**Table 2.** The expected numbers of SNe Ia within the JADES survey area in 1 year. See text for explanation.

## REFERENCES

- Barbary, K., Barclay, T., Biswas, R., et al. 2016, SNCosmo: Python library for supernova cosmology, *Astrophysics Source Code Library*, record ascl:1611.017
- Brachetti, P., De Felice Ciccoli, M., Di Pillo, G., & Lucidi, S. 1997, *J. Glob. Optim.*, 10, 165, doi: [10.1023/A:1008250020656](https://doi.org/10.1023/A:1008250020656)
- Brout, D., Scolnic, D., Popovic, B., et al. 2022, *ApJ*, 938, 110, doi: [10.3847/1538-4357/ac8e04](https://doi.org/10.3847/1538-4357/ac8e04)
- Chatzopoulos, E., Wheeler, J. C., Vinko, J., Horvath, Z. L., & Nagy, A. 2013, *ApJ*, 773, 76, doi: [10.1088/0004-637X/773/1/76](https://doi.org/10.1088/0004-637X/773/1/76)
- Eisenstein, D. J., Willott, C., Alberts, S., et al. 2023, arXiv e-prints, arXiv:2306.02465, doi: [10.48550/arXiv.2306.02465](https://doi.org/10.48550/arXiv.2306.02465)
- Foreman-Mackey, D. 2016, *The Journal of Open Source Software*, 1, 24, doi: [10.21105/joss.00024](https://doi.org/10.21105/joss.00024)
- Kenworthy, W. D., Jones, D. O., Dai, M., et al. 2021, *ApJ*, 923, 265, doi: [10.3847/1538-4357/ac30d8](https://doi.org/10.3847/1538-4357/ac30d8)
- Kessler, R., & Scolnic, D. 2017, *ApJ*, 836, 56, doi: [10.3847/1538-4357/836/1/56](https://doi.org/10.3847/1538-4357/836/1/56)
- Lu, J., Wang, L., Chen, X., et al. 2022, *ApJ*, 941, 71, doi: [10.3847/1538-4357/ac9f49](https://doi.org/10.3847/1538-4357/ac9f49)
- Oda, T., & Totani, T. 2005, *ApJ*, 630, 59, doi: [10.1086/431748](https://doi.org/10.1086/431748)
- Pierel, J. D. R., Jones, D. O., Kenworthy, W. D., et al. 2022, *ApJ*, 939, 11, doi: [10.3847/1538-4357/ac93f9](https://doi.org/10.3847/1538-4357/ac93f9)
- Pierel, J. D. R., Engesser, M., Coulter, D. A., et al. 2024, *ApJL*, 971, L32, doi: [10.3847/2041-8213/ad6908](https://doi.org/10.3847/2041-8213/ad6908)
- Regős, E., & Vinkó, J. 2019, *ApJ*, 874, 158, doi: [10.3847/1538-4357/ab0a73](https://doi.org/10.3847/1538-4357/ab0a73)
- Riess, A. G., Yuan, W., Macri, L. M., et al. 2022, *ApJL*, 934, L7, doi: [10.3847/2041-8213/ac5c5b](https://doi.org/10.3847/2041-8213/ac5c5b)



Rodney, S. A., Riess, A. G., Strolger, L.-G., et al. 2014, AJ, 148, 13, doi: [10.1088/0004-6256/148/1/13](https://doi.org/10.1088/0004-6256/148/1/13)

Scolnic, D., Brout, D., Carr, A., et al. 2022, ApJ, 938, 113, doi: [10.3847/1538-4357/ac8b7a](https://doi.org/10.3847/1538-4357/ac8b7a)

Scolnic, D. M., Jones, D. O., Rest, A., et al. 2018, ApJ, 859, 101, doi: [10.3847/1538-4357/aab9bb](https://doi.org/10.3847/1538-4357/aab9bb)

Tripp, R. 1998, A&A, 331, 815

Yan, H., Wang, L., Ma, Z., & Hu, L. 2023, ApJL, 947, L1, doi: [10.3847/2041-8213/acc93f](https://doi.org/10.3847/2041-8213/acc93f)